

# Experimental Performance Investigation of Photovoltaic Module and Water Cooled Photovoltaic/Thermal System under Middle of Iraqi Climatic Conditions

Haroun Shahad\*<sup>1</sup>, Mohammed Hasan Abbood<sup>2</sup>, ZuhairJeburDakhil<sup>3</sup>

<sup>1</sup>University of Babylon, <sup>2,3</sup>University of Kerbala  
\*Corresponding Author Email: [hakshahad@yahoo.com](mailto:hakshahad@yahoo.com)

## Abstract

Photovoltaic(PV) cells are one of the most important resources of renewable energy. In this paper, an experimental comparative performance study between PV module and water-cooled photovoltaic/thermal (PV/T) solar system at different flowrates of (0.5, 1, 1.5, 2) L/min is presented and including their thermal and electrical performances. The experiments were carried out under outdoor exposure to the climate of Hilla, Iraq (32.46 °N, 44.42 °E). Solar irradiance, the temperatures on the front surfaces and back sheet of PV and PV/T solar system, flowing water, ambient air and wind speed are measured. In addition, the electrical power of PV module and PV/T solar system is measured.

The results show that the maximum enhancement ratio of electrical efficiency of the PV/T solar system compared with PV module is 18.86% in March at flowrate of 2 L/min. The minimum enhancement is 13.36 % in July at flowrate of 0.5 L/min. The maximum overall efficiency improvement ratio of PV/T solar system compared to PV module is 81% in March at flowrate of 2 L/min while the minimum improvement is 74.08% in July at a flowrate of 0.5 L/min. The maximum average of cooling water temperature rise is 11.28 °C at a flowrate of 0.5 L/min in March, while the minimum is 2.69 °C at a flowrate of 2 L/min in July.

**Keywords:** Solar energy, PV/T solar system, PV module, experimental investigation, comparative study, performance, cooled water.

## 1. Introduction

Due to the growing environmental concerns and the depletion of fossil fuel, the world is paying more regard to use of renewable energy. Solar energy appears to be more promising and Sustainable energy resource (Tiwari *et al.*, 2009).

Today, Photovoltaic (PV) cell is one of the fastest growing renewable energy technologies. According to renewable global status report 2016, the global energy production with PV modules reached to 230 GW and installed capacity is projected to be beyond 500 GW in 2020 (Sathe and Dhoble, 2017).

Photovoltaic technology has been developing quickly and studies showed that only less than 20% of solar energy could be converted into electricity while the rest being wasted as heat. This heat raises the temperature of PV cells. Efficiency of PV cell decreases by about (0.4-0.65)% at increment one degree °C of temperature rise (Brahim and Jemni, 2017).

The concept of hybrid photovoltaic/thermal (PV/T) solar system refers to use PV module as part of the thermal collector, where PV module is cooled by circulating fluid to reduce its temperature and improve its performance, and benefit from extracted heat to increase the total efficiency of the system (Brahim and Jemni, 2017).

PV/T solar system produces heat and electricity simultaneously where the PV module produces electrical power, but acts also as a heat absorber surface to transfer the heat for various applications like space heating, industrial process of heating and preheating, crop drying and so on. A PV/T solar system can work with a

medium temperature of (60 - 80°C) and suitable electrical efficiency (Ibrahim *et al.*, 2011).

The PV/T systems are classified depends on the type of fluid used, the shape of the system, the type of the collector used, integrated into a building or not, existence of glazing on the system and a PV/T solar system's characteristics (Sathe and Dhoble, 2017).

The history of hybrid systems began with the work of Wolf Kern and Russell in the middle of 1970s. Many experimental studies done in recent years to develop and improve the efficiency of PV/T solar systems. Conventionally, air and water are being used as a thermal fluid in PV/T solar systems. Al harbiet al., reported that the electrical power generation of PV module decreased more than 30% in summer compared to that power generation during winter in Saudi Arabia. Sopian *et al.*, 2000 developed and tested a double pass photovoltaic thermal solar system suitable for solar drying applications. Ocampo *et al.*, 2007 reported that the hybrid system implemented with a bifacial module produces a large amount of electrical energy than a conventional PV/T solar system by 40% approximately. Fudholi *et al.*, 2013 showed the spiral absorber water PV/T solar system produced the best electrical efficiency and a thermal efficiency of other absorbers. Othman *et al.*, 2015 proposed a design of a solar system that is able to provide both hot water and hot air to improve the annual thermal conversion ratio of solar energy.

The water PV/T solar system consists of the same parts that used in the water solar collector with the PV module is installed on top of the collector (Hasan and Sumathy, 2010).

The water PV/T solar system more efficient compared to the air PV/T solar system due to the better thermo-physical properties

compared to air, but the air based most practical due to the minimum operational cost. (Chow, 2010).

The objective of the present work is to compare the performance of water PV/T solar system with PV module under Iraq climatic conditions. The performance of water PV/T solar system includes the electrical efficiency ( $\eta_e$ ) and the thermal efficiency ( $\eta_{th}$ ). The electrical efficiency ( $\eta_e$ ) of the PV module is the ratio of the maximum electrical power ( $P_m$ ) produced by the module to solar irradiance. The thermal efficiency of water PV/T solar system is the ratio of the maximum useful heat energy generated by the module to solar irradiance. The efficiencies are calculated by equations below (Zondag *et al.*, 2002):

$$\eta_e = P_m / (SR A_{ce}) \tag{1}$$

$$\eta_{th} = \dot{m} c_f (T_{fo} - T_{fi}) / (SR A_{ce}) \tag{2}$$

Where: SR is solar irradiance,  $A_{ce}$  is area of solar cell,  $\dot{m}$  is mass flowrate,  $c_f$  is heat capacity of cooling water,  $T_{fo}$  is temperature of outlet cooling water and  $T_{fi}$  is temperature of inlet cooling water. The overall efficiency ( $\eta_o$ ) is combined of thermal efficiency and electrical efficiency as below:

$$\eta_o = \eta_e + \eta_{th} \tag{3}$$

## 2. Experimental Work

A special experimental rig is constructed to study the performances of water PV/T system and PV module. It comprises from the following parts:

1. Two PV module type ISP100 used in this study as shown in Figure (1a).

2. One of PV modules is modified to be a PV/T system by attaching a cooling pocket to the whole area of its backside. The pocket is made of Acrylic (glass plastic) with thickness (6 mm) with a depth of (7 mm). The cooling water enters at the bottom and leaves at the top. The cooling water is in direct contact with the back sheet of the PV module that used in the PV/T system as shown in Figure (1b).

3. A thermal insulator from polystyrene board (foam) with thickness (50 mm) to minimize the back and side losses is used.

4. Frame and sections of aluminium are manufactured to support the water pocket and contains the insulation layer and thermocouples used for temperature measurement, as shown in Figure (1 b and c).

The cooling water is directly contact with the back sheet of PV module that used in PV/T solar system. 3. A thermal insulator from polystyrene board with thickness (50 mm) to minimize the back losses.

4. Frame and sections of aluminium are manufactured to base Water channel and contained the insulation layer and thermocouples, which placed on the back sheet of PV module as shown in Figure (1c).

5. Two steel structures are designed to support the PV module and PV/T solar system at the chosen tilt angle (35° in March and 11.5° in July) and stationary south facing.

6. Two insulated plastic tanks of 500 litter with insulated plastic pipes to supply the cooling water at constant head to PV/T system to get the required volume flowrate.

Figure (2) shows the schematic diagram of PV/T solar system, while Figure (3) shows the different parts of the rig. The technical specification of materials of rig and technical data of PV module used in this work are given in Tables (1) and (2) respectively. Figure (4) shows locations of thermocouple node. The tests have been taken at a different volume flowrate (0.5, 1, 1.5 and 2) litre/min, each day one flowrate.



a:PV module b:Channel of Cooling Water c:Back Side of PV/T System  
**Fig. 1: PV Module and Parts of PV/T Solar System**

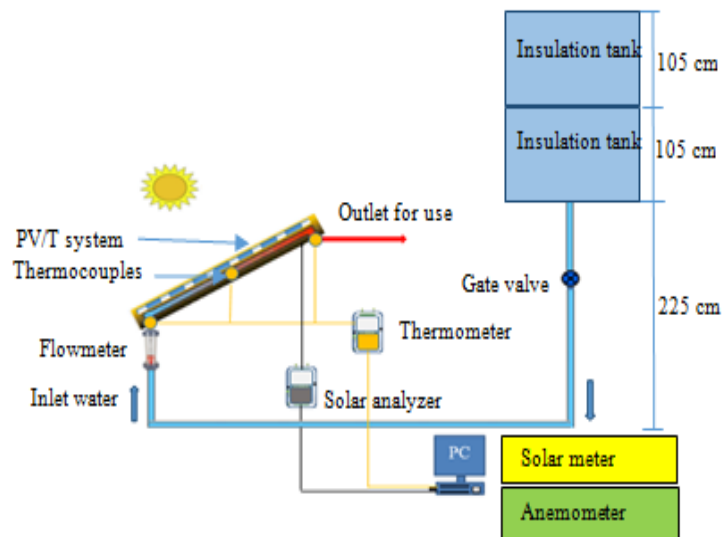


**Fig. 2: Schematic Diagram of PV/T Solar System**

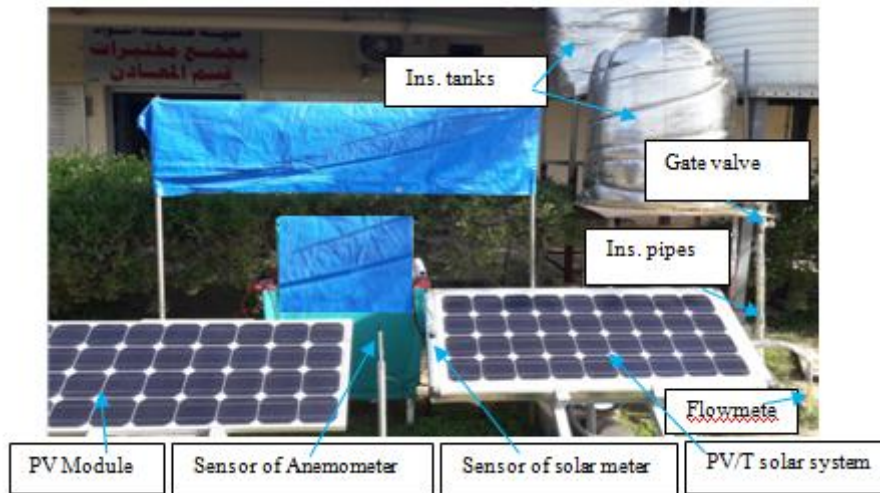


Fig. 3: Parts and Details of Experimental Rig

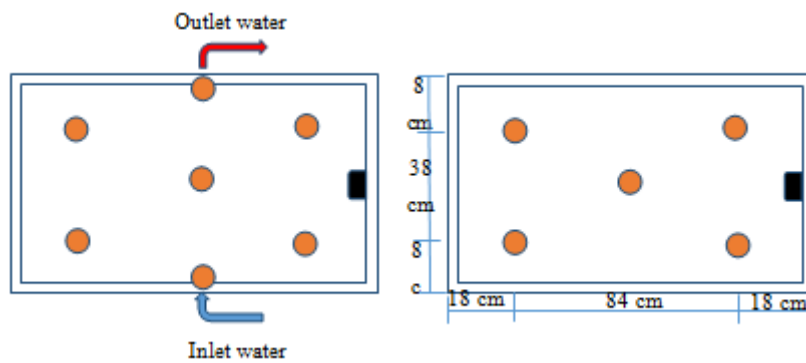


Fig. 4: Schematic Diagram of Locations of Thermocouples

Table 1: Technical Specification of Materials of Rig at (20°C)

Material	Thermal conductivity W/(m .°K)	Heat capacity kJ/ (kg. °K)	Density kg/m <sup>3</sup>
Water	0.591	4.184	997.04
Polystyrene board(foam)	0.03	1.3-1.5	32-35
Acrylic(glass plastic)	0.19	1.46	1180
Aluminium	237	0.902	2700

Table 2: Electrical and Technical Data of PV Module at Standard Testing Condition

Model of Module	Is100p Mono	Open circuit voltage	22 Volts
Peak power	100 Watts	Voltage at max. power	17.8Volts
No. cell	36	Nominal temperature	45±(2) °C
Dimension of cell	125*125 mm	Temperature cell range	- 40 to +85 °C
Nominal Voltage	12 Volts	Dimensions of Module	1200*540*40 mm
Current at max. power	5.62 Ampere	Weight	9.3 kg
Short Circuit Current	6.15 Ampere	Power tolerance	± 3%

### 3. Measurement Instruments

They following instrumentations are used in this work:

1. Thermometer, type Lutron BTM-4208SD, a digital and 12 channel with SD card is used to record the temperature of the inlet and outlet water and the backside of the PV cells.
2. Twelve calibrated thermocouple, type k, Nickel Chrome/Nickel Aluminium are used to measure the temperatures. Ten of them are distributed on the backside surface of the panels and two are fixed on the inlet and outlet of cooling.
3. Hot wire Anemometer, type Lutron YK-2005AM is used to record the ambient temperature and wind speed.
4. Thermal camera, type FLIR i5 is used to measure the temperature of the front surface of PV module and PV/T system.
5. Solar Module Analyzer, type PROVA 200A is used to record the characteristic voltage, current and power of the PV module and PV/T system.
6. Solar meter, type TES 132 is used to measure solar irradiance.

7. A Flow meter, type SHLLJ is used to measure the flowrate of cooling water range (1-8) litter /min.

The range, resolution and accuracy of the instrumentations are shown in Table (3).

Table 3: Range, Resolution and Accuracy of Instrumentations

Instrument	Measurement	Range	Resolution	Accuracy
Thermometer Type Lutron BTM-4208SD (type k)	Temperature	-50.0 to 999.9 °C	0.1 °C	± ( 0.4 % + 1 ) °C
Hot Wire Anemometer Type Lutron YK-2005AM (type k)	Air speed	0.2 to 20.0 m/s	0.1 m/s	± ( 5 % + 0.1 ) m/s
	Air Temperature	-50.0 to 1300.0 °C	0.1 °C	± 0.8 °C
Solar	Voltage	10-	0.01V	±1%±

Module Analyzer Type PROVA 200A.	Current	60V	0.001A	(1% $V_{oc} \pm 0.09$ ) V
		0-1A		$\pm 1\% \pm (1\% I_{sh} \pm 0.009)$ A
Solar Meter Type TES 132	Solar radiation	0 to 2000 W/m <sup>2</sup>	0.1W/m <sup>2</sup>	$\pm 5\% \pm 0.38$ W/m <sup>2</sup> /°C from 25 °C
Thermal Camera Type FLIR i5	Temperature	0 to 250°C	80×80 pixels	$\pm 2\%$ °C of reading

temperature measurements, electrical measurements and performance measurements as below:

### 4.1 Temperature Measurement Results

Figure(5) shows the variation of ambient air temperature and solar irradiance with time during the test days with clear sky conditions.

The ambient air temperature follows the incident solar radiation from sunrise to solar noon, after which a considerable deviation in its behavior is indicated. It is noted that on 12 March, the ambient air temperature is about 30°C, while on 2 July the maximum ambient air temperature is upper 45 °C.

Figure (6) shows the variation of ambient air temperature and wind speed with time for selected clear days during the test period. The ambient air temperature decreases with increasing wind speed and then effect of wind speed decreases when ambient air temperature continuous by raising result of accumulating the heat energy in the ground.

## 4. Results and Discussion

The experiments were carried out under outdoor exposure conditions under the climate of middle Iraq (Hilla city) within the University of Babylon Campus, located at 32.46 °N, 44.42°E. The effect of cooling on electrical and thermal performance of PV Module has been studied. The experimental results include

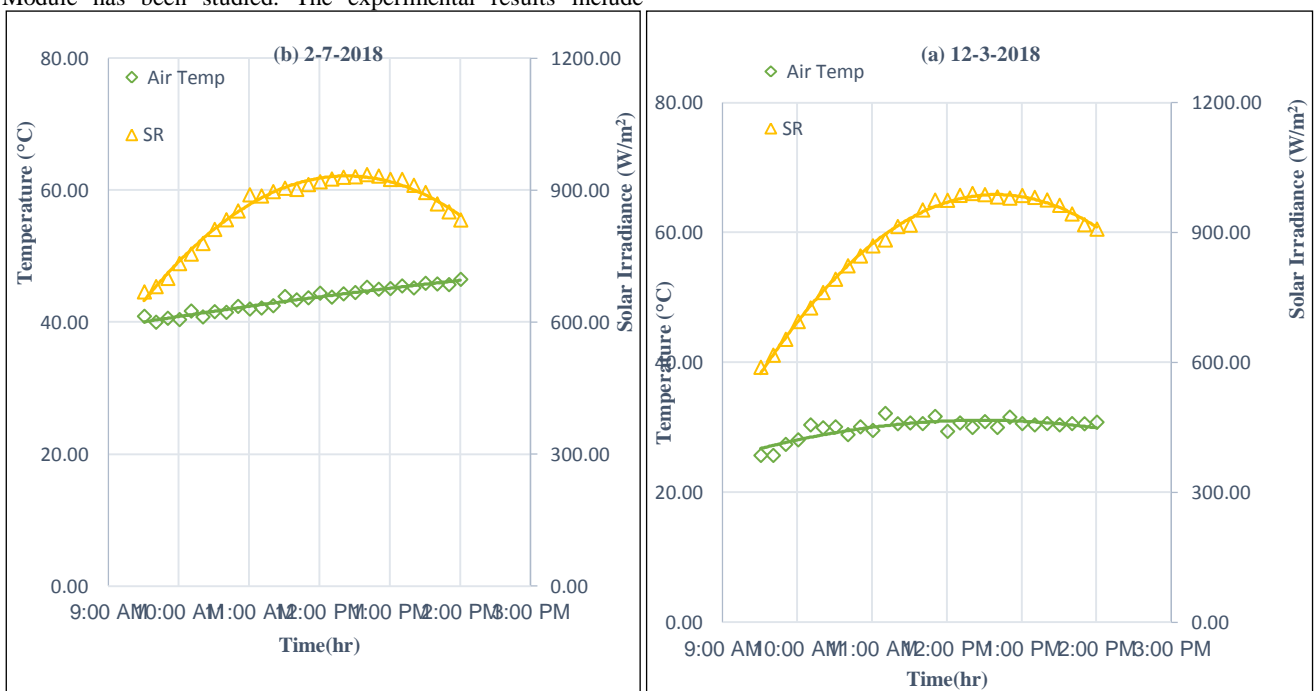
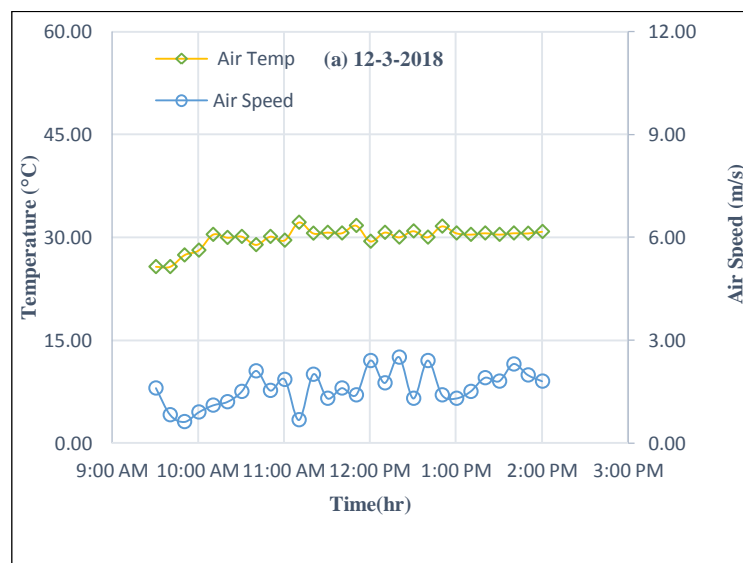


Fig. 5: Ambient air Temperature and Solar Irradiance with Time for Selected Day from 2018



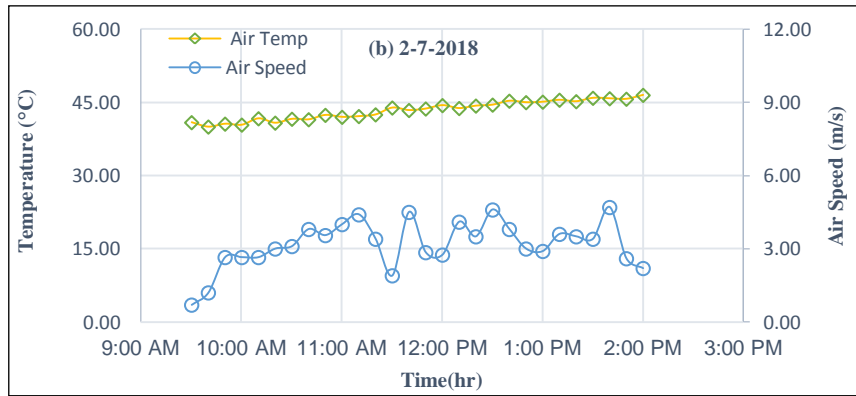


Fig. 6: Ambient Air Temperature and Air speed with Time for Selected Days from July 2018

Figure(7) shows that the average temperature of the back sheet of PV module follows the trend of solar irradiance. The figure also shows the back sheet temperature of the PV/T system. It is shown the maximum back sheet average temperature of PV module rises to about 59.47°C for 12 March 2018 and 68.26°C for 2 July 2018,

while for the PV/T system, it drops to 32.35°C and 49.7°C at inlet cooling water temperature of 20.05°C and 35.8°C respectively and flow rate of 1.5 L/min. It is clear that cooling has significant effect on back sheet temperature.

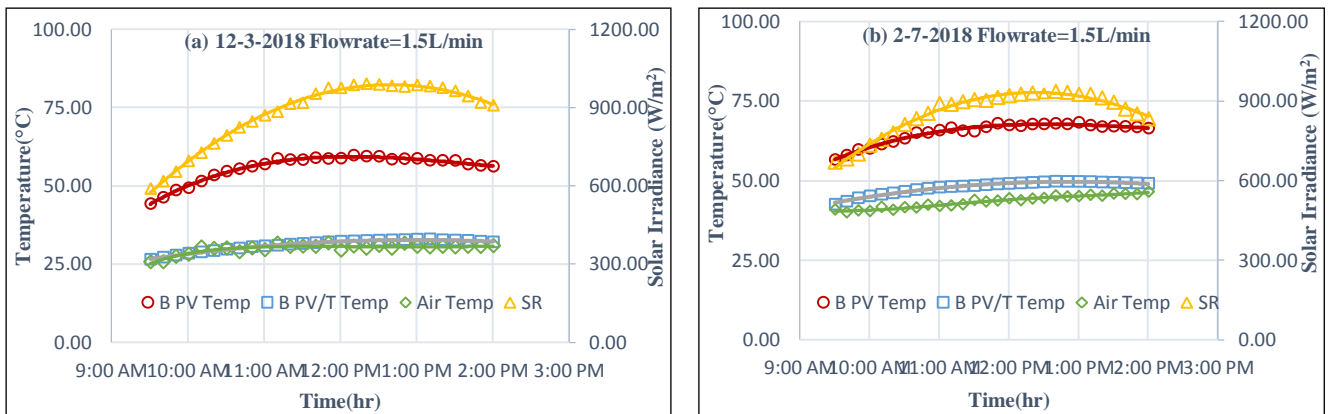


Fig. 7: Temperatures Average of Back Sheet of PV Module and PV/T System, Ambient Air Temperature and Solar Irradiance with Time for Selected Day from 2018

Figure (8) shows that the daily average temperature of the back sheet of a PV module is higher than that of the PV/T system for all tests and the temperatures in July are higher than in March. The maximum daily average temperature of PV module is 66.86°C on 4 July, while the minimum temperature is 55.93°C on 12 March. The maximum daily average temperature of PV/T solar system is 48.89°C on 4 July at a flow rate of 0.5m L/min, while the minimum temperature is 30.52 °C on 13 March at a flow rate of 2 L/min. Figure (9) illustrates the temperatures of the middle region

of the front surface of PV module and PV/T solar system. The results show a clear difference in temperature due to cooling. It is noticed that there is a gradient of temperature in the directions of cooling water flow and current flow along with the module. It is also noticed that the temperature of front surface is not uniform where there are low temperature regions due to the packing effect. In addition, the temperatures of front surface of PV module is lower than temperatures of back sheet.

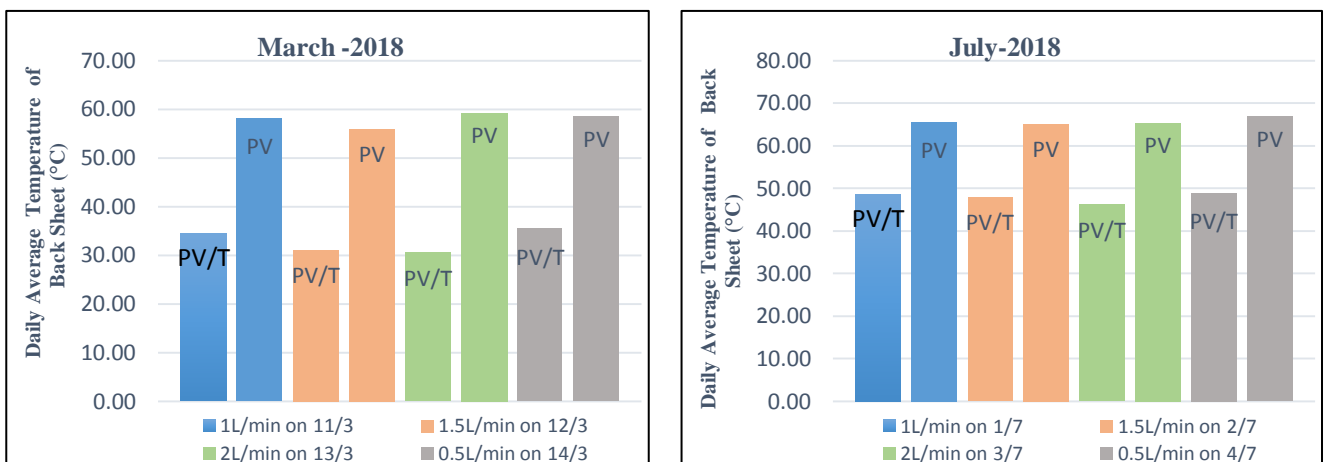
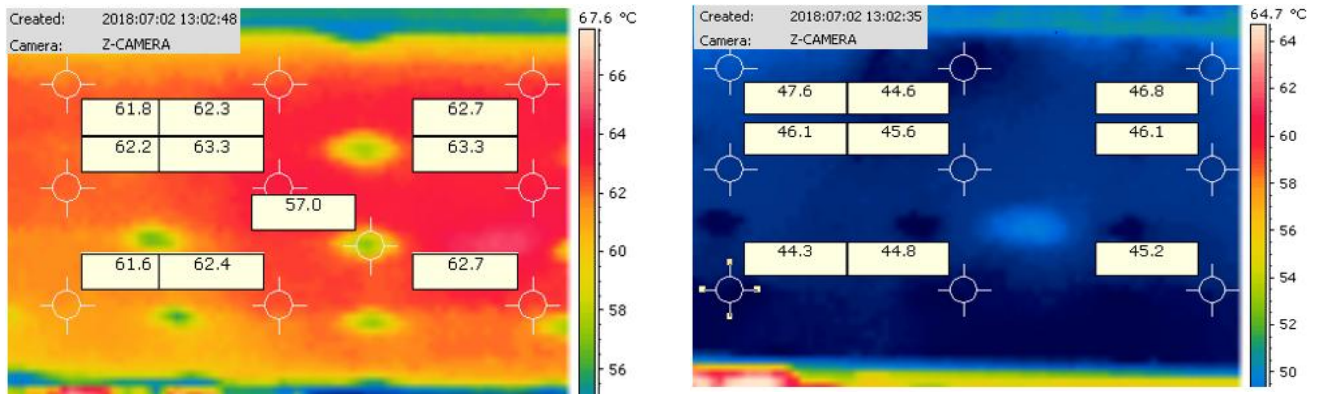


Fig. 8: Daily Average Temperatures of Back Sheet of PV Module and PV/T System for Selected Days from 2018

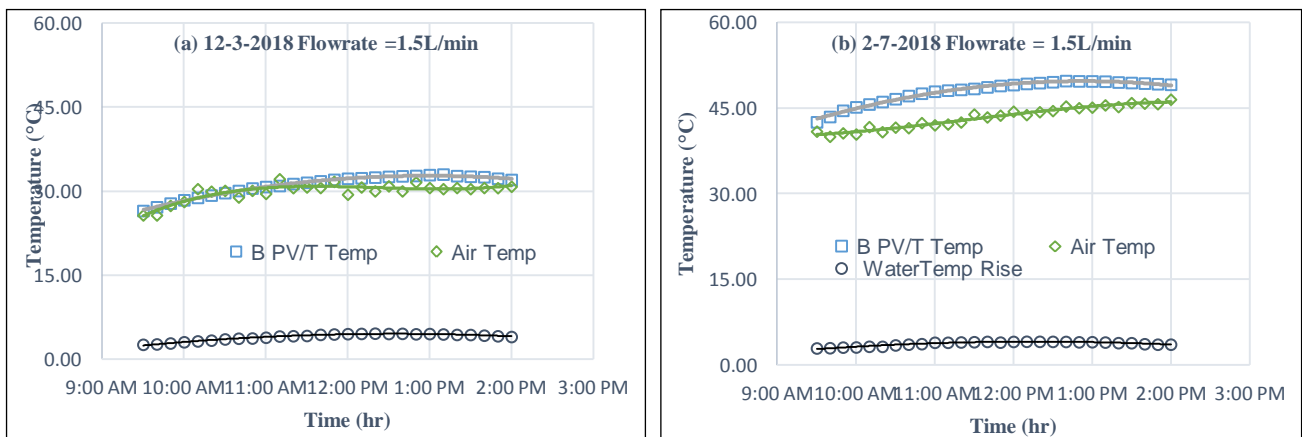




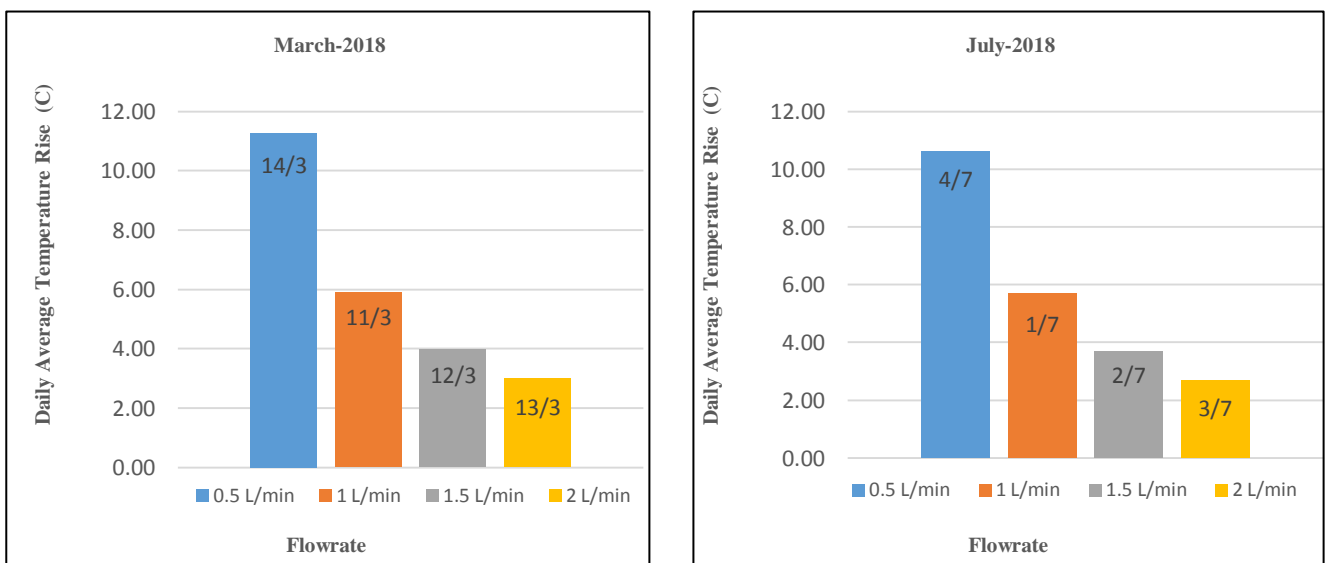
a:PV Module b:PV/T Solar System  
**Fig. 9:** Front surface Temperature for 2 July 2018

Figure (10) shows that the time variation of temperature rise of cooling water during the day for 12 March and 2 July 2018. It is seen that the temperature difference increases slightly with time and then decreases. The maximum temperature difference of flowing water is at noon and it is less in July as a result of increasing the heat losses due to increase the temperature of the back sheet of PV cells above ambient temperature and high inlet water temperature. The daily temperature average of inlet water about 20.05°C on 12 March and 35.8°C on 2 July.

Figure (11) illustrates the average temperature rise of cooling water on it flows along the back sheet of the panel during selected days from March and July 2018. Temperature rise of flowing water in March is higher in July for same flow rate due to the lower inlet temperature compared to March. The maximum average temperature rise of cooling water is 11.28 °C in March at flow rate 0.5 L/min, while the minimum is 3°C at flow rate of 2 L/min. The maximum average temperature rise of cooling water is 10.62 °C in July at flow rate 0.5 L/min while the minimum is 2.69°C at flow rate of 2 L/min.



**Fig. 10:** Temperatures of Ambient Air, Back Sheet of PV/T System and Flowing Rise of Flowing Water with Time for Selected Days from 2018



**Fig. 11:** Daily Average of Temperature Rise of Flowing Water for Selected Days from 2018

### 4.2 Electrical Measurement Results

Figure (12) shows a comparison of PV/T solar system and PV module generated voltage at maximum power point ( $V_m$ ) during the day. The Figure shows that the  $V_m$  drops as time elapses due to increase the temperature. In all cases of tests, the  $V_m$  of PV/T solar system is higher than PV module and this difference increases with increasing the flowrate of cooling water because of decreasing the temperature of PV cells.

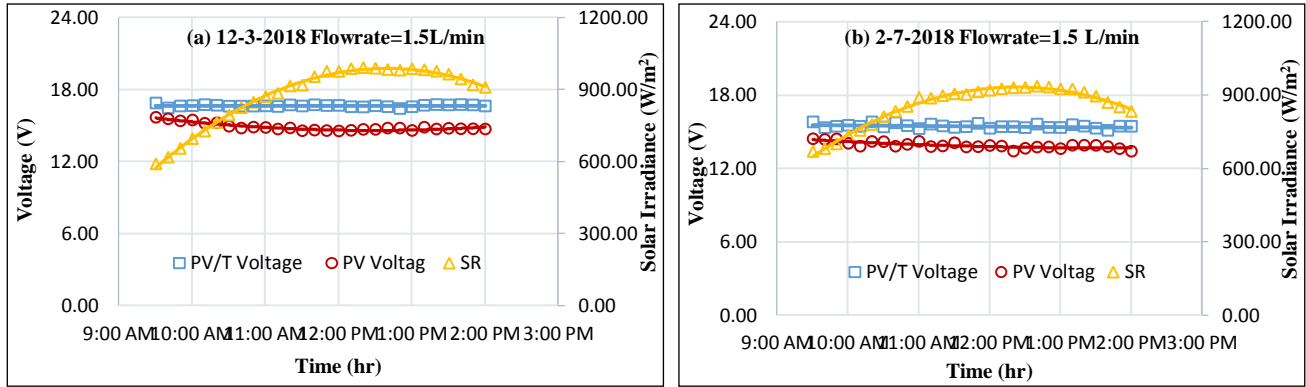


Fig. 12: Voltage of PV Module and PV/T System at Maximum Power Point and Solar Irradiance with Time for Selected Days from 2018

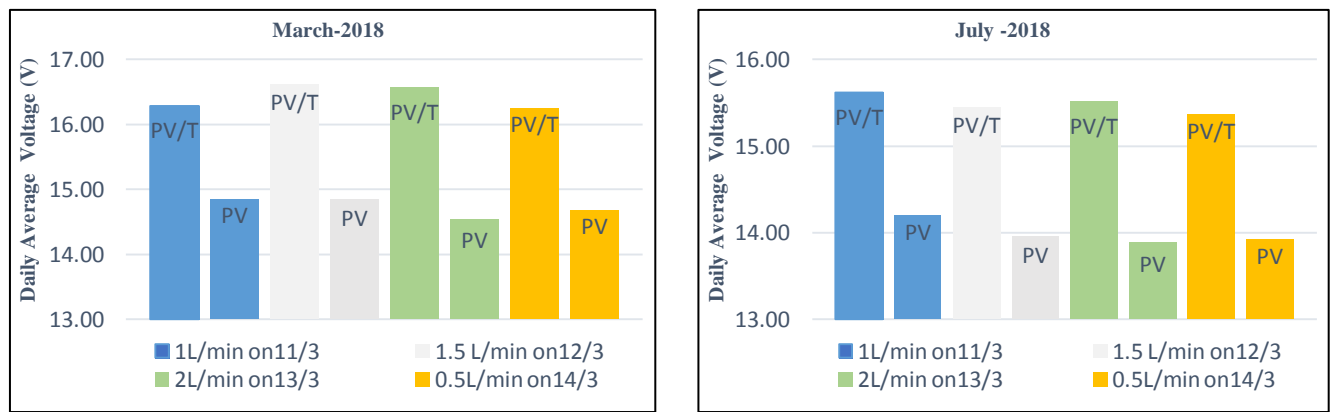


Fig. 13: Daily Voltages Average of PV module and PV/T Solar System at Maximum Power Point for Selected Days from 2018

Figure (14) shows that the current at maximum power point ( $I_m$ ) of PV follows the solar irradiance and increases with it. The  $I_m$  of PV/T solar system is more than  $I_m$  of PV module for all tests.  $I_m$  of

PV module and PV/T solar system increase with temperature of PV cells, where for most semiconductors, the bandgap energy decreases with increasing of temperature (Singh and Ravindra, 2012).

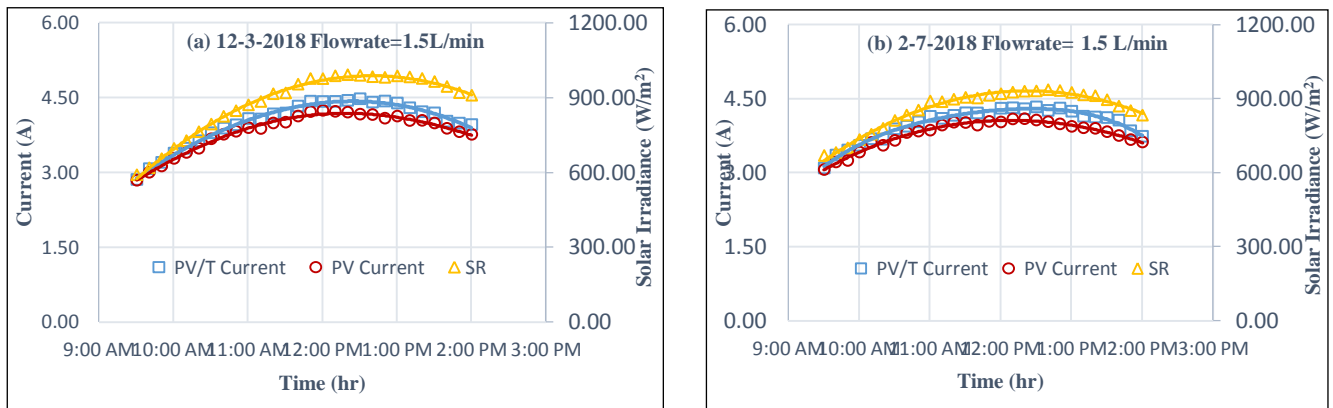


Fig. 14: The Current of PV Module and PV/T Solar System at Maximum Power Point and Solar Irradiance with Time for Selected Days from 2018

Figure (15) shows average  $I_m$  of PV/T solar system affect solar irradiance and water flowrate. The maximum daily average of  $I_m$  is

4 Ampere on 13 March with cooling, while the minimum is 3.59 Ampere on 4 July without cooling.

Figures (16) and (17) show the relationship between voltage and current, in addition with power for PV module and PV/T solar system respectively. The increase of current leads to decrease the

voltage and the maximum electrical power after maximum power point. The maximum electrical power, voltage and current of PV/T solar system are more than PV module for all cases of study.

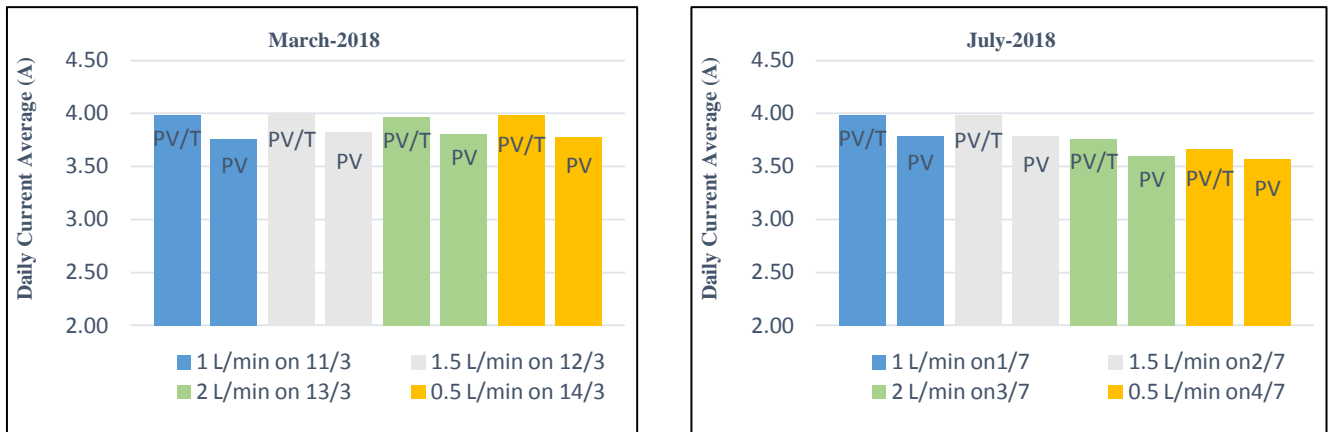


Fig. 15: Daily Current Average of PV Module and PV/T Solar System at Maximum Power Point for Selected Days from 2018

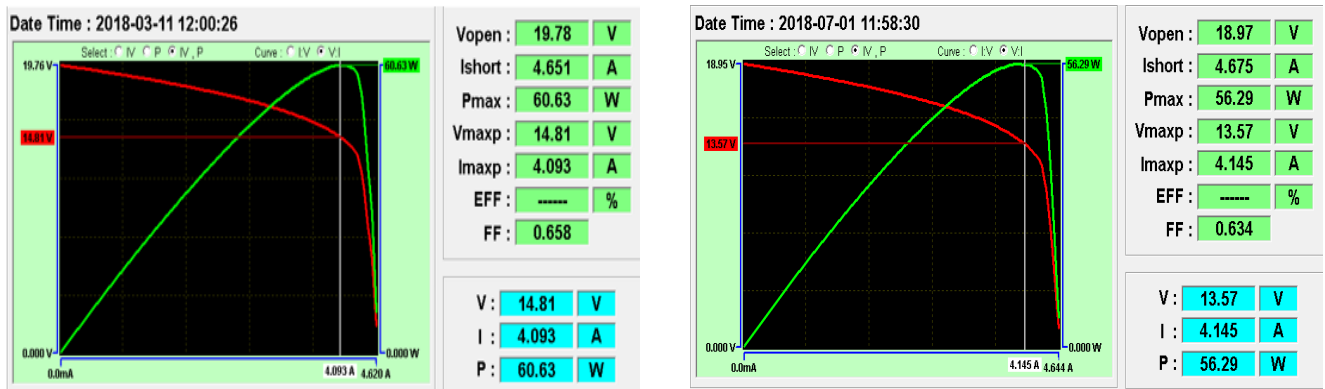


Fig. 16: The Characteristic Curves (I,V) and (I,P) of PV Module for Selected Days from 2018

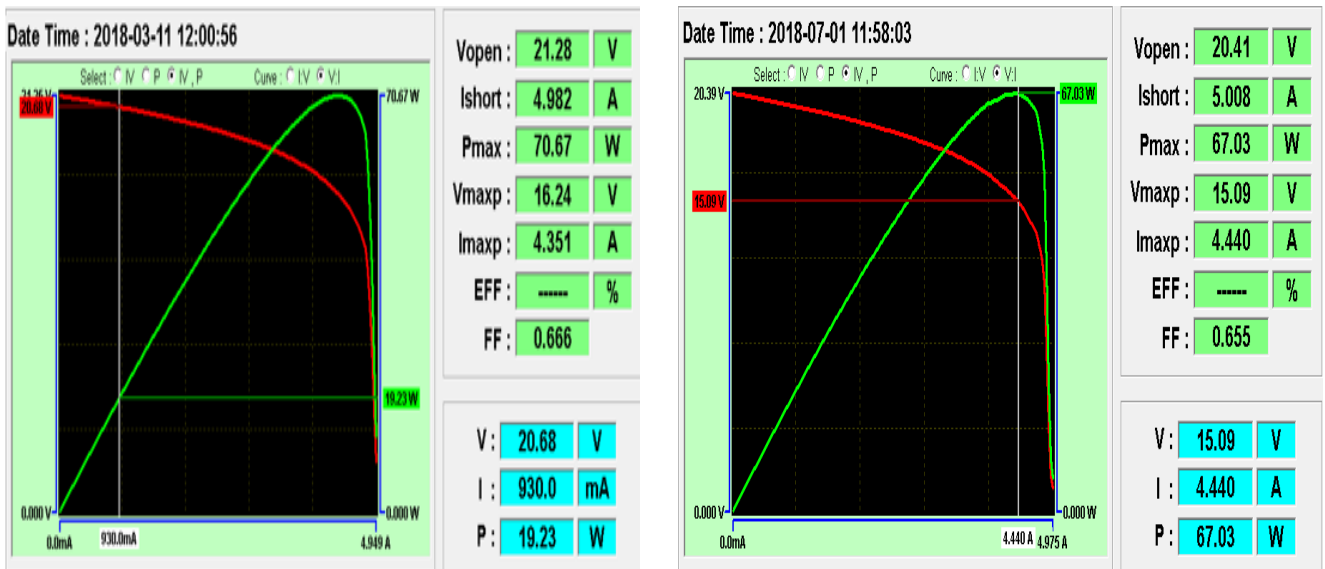


Fig. 17: The Characteristic Curves (I,V) and (I,P) of PV/T Solar System for Selected Day from 2018

Figure (18) shows that instantaneous maximum power ( $P_m$ ) of PV/T solar system is more than power of PV module for all tests, in addition, the  $P_m$  of PV module and PV/T solar system is higher in March than July due to higher cells temperature in July. The instantaneous maximum power follows solar irradiance trends. Figure (19) shows that the daily average electrical power of PV module and PV/T solar system in winter is better than summer because of increasing the temperature of PV cells that leads to

reduce band gap energy (Tobnaghi *et al.*, 2013). The daily average  $P_m$  maximum of PV/T solar system is 66.53 Watt and the minimum is 63.25 Watt in March, while the maximum is 62.21 Watt and the minimum is 56.29 Watt in July. The  $P_m$  maximum daily average of PV module is 56.63 Watt and the minimum is 55.17 Watt in March, while the maximum is 53.67 Watt and the minimum is 49.61 Watt in July.



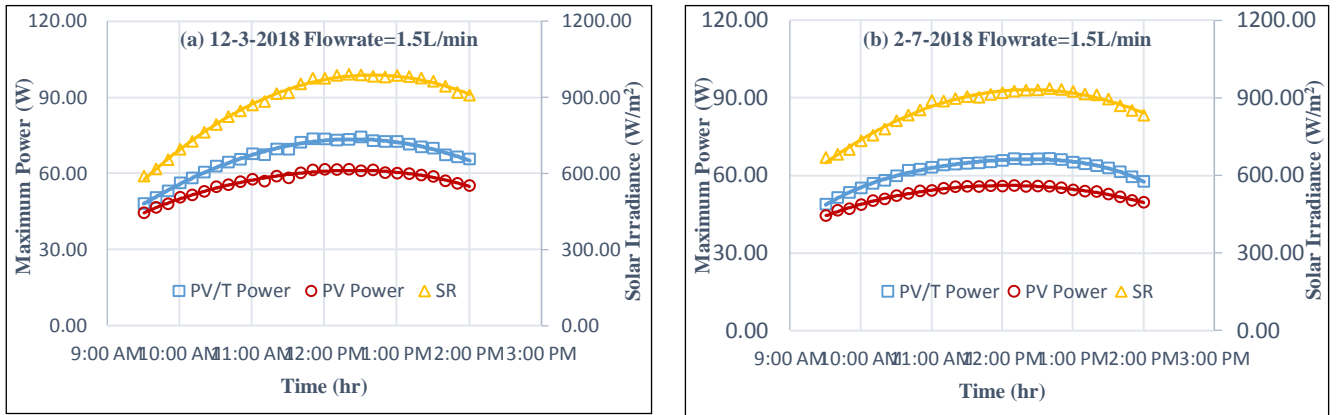


Fig. 18: Maximum Electrical Power of PV Module and PV/T Solar System and Solar Irradiance with Time for Selected Days from 2018

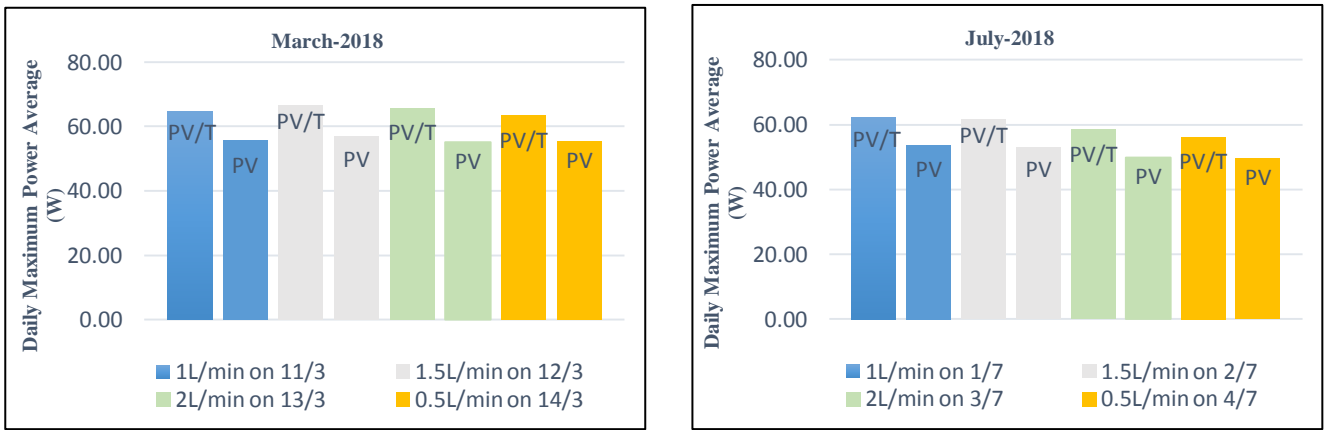


Fig. 19: Daily Average of Maximum Electrical Power of PV module and PV/T Solar System for Selected Days from 2018

### 4.3 Performance Measurement Results

Figure (20) shows that the electrical efficiency of PV/T solar system is more than electrical efficiency of PV module for all cases and this difference increases with increasing the flowrate of following water vice versa. The instantaneous electrical efficiency decreases with increase of solar irradiance result of increase the temperature of PV cells with solar irradiance that leads to reduce

the production of electrical power in proportion to amount of solar irradiance.

Figure(21) shows that the enhancement ratio of electrical efficiency in the winter is more than summer because of the high temperature of PV cells and cooling inlet water. The maximum enhancement ratio of electrical efficiency is 18.86% on 13 March at flowrate of 2L/min, while the minimum is 13.36% on 4 July at flowrate of 0.5L/min.

Where:  $\text{efficiency enhancement ratio} = \frac{(\text{maximum efficiency} - \text{minimum efficiency})}{(\text{minimum efficiency})}$

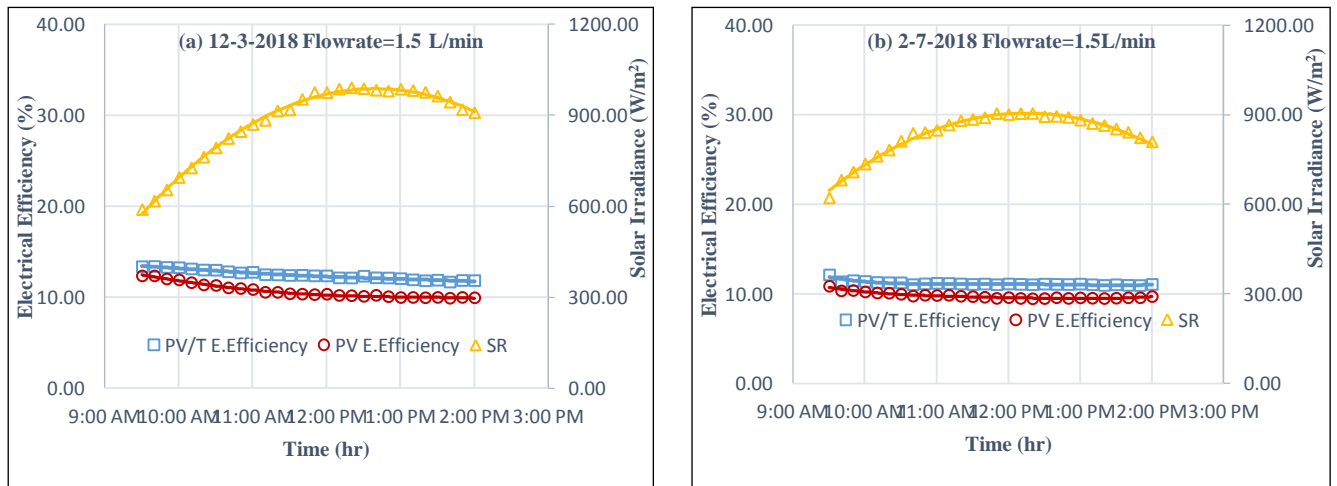


Fig. 20: Electrical Efficiency of PV Module and PV/T System and Solar Irradiance with Time for Selected Days from 2018

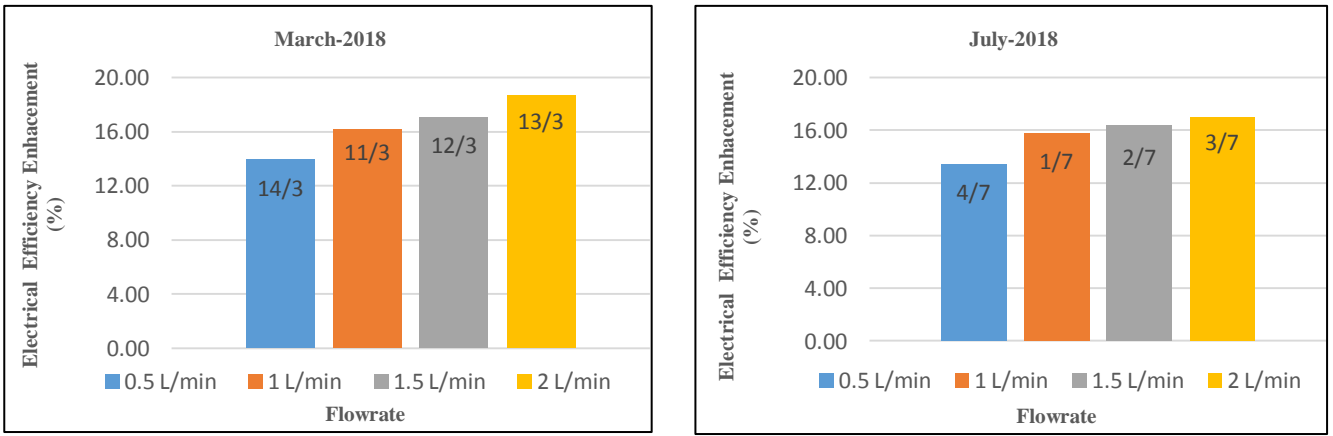


Fig. 21: Electrical Efficiency Enhancement of PV/T Solar System Compared to PV Module for Selected Days from 2018

The instantaneous overall efficiency of PV/T solar system throughout the day is shown in fig (22) together with the instantaneous efficiency of PV module. It is shown that the overall efficiency of PV/T solar system is more than of PV module for all cases. This is due to the heat gained by cooling water. However, the instantaneous overall efficiency increase with increase of solar irradiance.

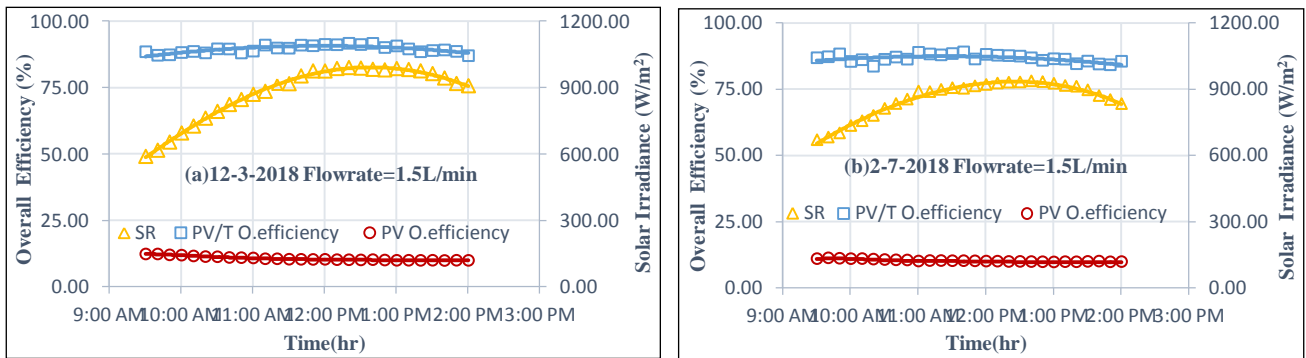


Fig. 22: Overall Efficiency of PV Module and PV/T Solar System and Solar Irradiance with Time for Select Days from 2018

Figure (23) shows that a daily average of overall efficiency increase in the winter is better than in summer. This may be attributed to high electrical efficiency in winter and low inlet water

temperature. The maximum increase of overall efficiency is 81% on 13 March at flowrate of 2 L/min, while the minimum is 74.08% on 4 July at flowrate of 0.5 L/min.

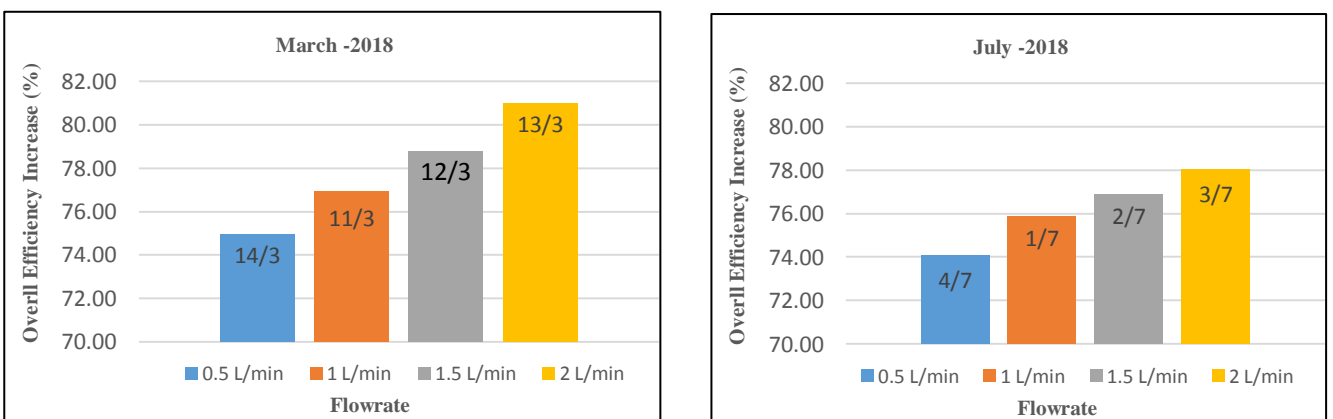


Fig. 23: Daily Increase of Overall Efficiency of PV Module Compared to PV/T Solar System for Selected Days from 2018

### 5. Conclusions

The conclusions of this work is summarized below:

- The generated electrical power drops with the increase of PV module temperature, which is affected by solar irradiance, ambient temperature and wind speed.
- The maximum temperature average of back sheet with and without cooling occurs in July and the minimum occurs in

March. The maximum daily average of temperature difference between them is 28.7 °C on 13 March at a flowrate of 2 L/min.

- The temperature of front surface of PV module is higher than temperature of front surface of PV/T solar system and it is lower than temperature of back sheet of PV module.
- The maximum average temperature rise of cooling water is 11.28 °C at flowrate 0.5 L/min in March, while the minimum is 2.69 °C at flowrate of 2 L/min in July.

- The maximum enhancement ratio of electrical efficiency of PV/T solar system compared with PV module is 18.86% in March at flowrate of 2 L/min. The minimum enhancement ratio is 13.36 % in July at flowrate of 0.5 L/min.
- The maximum overall efficiency increase of PV/T solar system is 81% compared to PV module March at flowrate of 2 L/min. The minimum increase is 74.08% in July at flowrate of 0.5 L/min.

## References

- [1] Brahim, T. and Jemni, A. (2017) 'Economical assessment and applications of photovoltaic / thermal hybrid solar technology: A review', *Solar Energy*. Elsevier Ltd, 153, pp. 540–561. doi: 10.1016/j.solener.2017.05.081.
- [2] Chow, T. T. (2010) 'A review on photovoltaic / thermal hybrid solar technology', *Applied Energy*. Elsevier Ltd, 87(2), pp. 365–379. doi: 10.1016/j.apenergy.2009.06.037.
- [3] Fudholi, A. et al. (2014) 'Performance analysis of photovoltaic thermal ( PVT ) water collectors', *Energy Conversion and Management*. Elsevier Ltd, 78, pp. 641–651. doi: 10.1016/j.enconman.2013.11.017.
- [4] Hamid, S. A. (2016) 'Performance analysis of PV / T Combi with water and air heating system: An experimental study', *Renewable Energy*. Elsevier Ltd, 86(October 2015), pp. 716–722. doi: 10.1016/j.renene.2015.08.061.
- [5] Harbi, Y. A. L., Eugenio, N. N. and Zahrani, S. A. L. (1998) 'RENEWABLE ENERGY', 5, pp. 5–8.
- [6] Hasan, M. A. and Sumathy, K. (2010) 'Photovoltaic thermal module concepts and their performance analysis: A review', *Renewable and Sustainable Energy Reviews*. Elsevier Ltd, 14(7), pp. 1845–1859. doi: 10.1016/j.rser.2010.03.011.
- [7] Ibrahim, A. et al. (2011) 'Recent advances in flat plate photovoltaic / thermal ( PV / T ) solar collectors', *Renewable and Sustainable Energy Reviews*. Elsevier Ltd, 15(1), pp. 352–365. doi: 10.1016/j.rser.2010.09.024.
- [8] Kern Jr. EC, Russell Mc., 1978, Combined Photovoltaic and Thermal Hybrid Collector System, Proceedings of 13th IEEE Photovoltaic Specialist pp.1153–7.
- [9] Sathe, T. M. and Dhoble, A. S. (2017) 'A review on recent advancements in photovoltaic thermal techniques'. Elsevier Ltd, (September). doi: 10.1016/j.rser.2017.03.075.
- [10] Singh, P. and Ravindra, N. M. (2012) 'Solar Energy Materials & Solar Cells Temperature dependence of solar cell performance — an analysis', *Solar Energy Materials and Solar Cells*. Elsevier, 101, pp. 36–45. doi: 10.1016/j.solmat.2012.02.019.
- [11] Sopian, K. et al. (2000) 'Performance of a double pass photovoltaic thermal solar collector suitable for solar drying systems', 41, pp. 353–365.
- [12] Tiwari, A. et al. (2009) 'Energy metrics analysis of hybrid – photovoltaic ( PV ) modules', *Applied Energy*. Elsevier Ltd, 86(12), pp. 2615–2625. doi: 10.1016/j.apenergy.2009.04.020.
- [13] Tobnaghi, D. M. and Madatov, R. (2013) 'The Effect of Temperature on Electrical Parameters of Solar Cells', pp. 6404–6407.
- [14] Trapaga, G., Javier, F. and Rodriguez, G. (2007) 'Photovoltaic / thermal solar hybrid system with bifacial PV module and transparent plane collector transparent plane collector', (February 2014). doi: 10.1016/j.solmat.2007.08.005.
- [15] Zondag, H. A. et al. (2002) 'The thermal and electrical yield of a PV-thermal collector', *Solar Energy*, 72(2), pp. 113–128. doi: 10.1016/S0038-092X(01)00094-9.